Extrapolation methods for accelerating unsteady partitioned fluid-structure interaction simulations

Stephen Sachs*, Marcel Streitenberger, Dörte C. Sternel, Michael Schäfer****
*Graduate School of Computational Engineering,
Technische Universität Darmstadt
**Fachgebiet Numerische Berechnungsverfahren im Maschinenbau,
Technische Universität Darmstadt

ABSTRACT

The advantages of an unsteady implicit partitioned Fluid-Structure Interaction Scheme are, especially for large time step sizes, accompanied by a high number of inner iterations needed. This work investigates the use of extrapolation techniques in between time steps to obtain a smaller number of inner iterations.

In contrast to previous works not only the structural displacement but also the fluid field variables are considered for extrapolation. The different extrapolation approaches are compared within a numerical benchmark.

Keywords: Fluid-Structure Interaction, Force Extrapolation

1. INTRODUCTION

In solving partitioned Fluid-Structure Interaction (FSI) problems, the implicit approach has shown great advantages in terms of time step restrictions and stability. Especially when exploiting its ability to use large time steps, a main challenge of this approach is to reduce the number of FSI iterations within every time step. This challenge has been investigated by numerous people.

Mainly the methods can be divided into two types. Methods working on acceleration within individual time steps and methods integrating several time steps. The former include, among others, adaptive under-relaxation of Aitken type as in [13, 6, 5, 14, 15, 9], reduced order modeling [13], steepest descent methods [5], or vector extrapolation [6].

Methods using multiple time steps are typically based on extrapolating the converged FSI solutions. Extrapolation in between time steps produce a more sophisticated first guess and thus reduce the number of FSI iterations needed in the current time step to reach convergence. This has been implemented into partitioned implicit [2] and partitioned explicit FSI solvers [3], but attention has been singly on the structural parameters as in [8, 9] or the displacement of the fluid field as in [14]. In [11] extrapolation has been implemented for the structural displacement and the fluid pressure.

This work introduces a method of force extrapolation. The extrapolation routines for the structural parameters are used for the fluid force acting on the structure at the FSI interface. Compared to the classical displacement extrapolation, the force extrapolation results in a greater acceleration. Furthermore, there are virtually no additional computational costs, as the same functions and memory blocks, as being used for the displacement, can be employed. Singly, one additional structure solution per time step is necessary.

In the following chapter, the underlying conservation equations are given in the Arbitrary Lagrangian-Eulerian formulation (ALE), then the native FSI algorithm is introduced. Thereafter the extrapolation functions are presented as well as the implementation for displacement and force extrapolation. After specifying the underlying solution software and the FSI test case, numerical results of all implementations are shown and compared for 3 different time step sizes.

2. FLUID-STRUCTURE INTERACTION SYSTEM

In the following a subscript f refers to the fluid and a subscript s to the structure. Let Ω be our computational FSI domain described in the ALE framework, which has a disjoint partition into the structure domain Ω_s and the fluid domain Ω_f with FSI boundary $\Gamma = \overline{\Omega_s} \cap \overline{\Omega_f}$. Let the velocity and pressure denoted by $(v,\ p)$ be well defined with all boundary conditions on the respective remaining boundaries $\partial\Omega_f \setminus \Gamma$. Then, the fluid part of the coupled problem can be stated as the Navier-Stokes equations for incompressible Newtonian fluids in the ALE framework

$$\frac{\partial}{\partial t}\int_{\Omega_f} \rho_f v\, dV + \int_{\partial\Omega_f} \rho_f \left(v - v^g\right) v n\, dA = \int_{\partial\Omega_f} \sigma n\, dA + \int_{\Omega_f} \rho_f f_f dV \ \text{ in } \Omega_f \quad (1)$$

$$\frac{\partial}{\partial t}\int_{\Omega_f} \rho_f dV + \int_{\partial\Omega_f} \rho_f \left(v - v^g\right) n\, dA = 0 \ \text{ in } \ \Omega_f \quad (2)$$

with v^g the ALE grid velocity, ρ_f the fluid density, n the outer normal vector, f_f outer forces acting on the fluid,

$$\sigma_f = \mu_f \left(\nabla v + \nabla v^T\right) - pI \quad (3)$$

the Cauchy stress tensor, p the pressure, I the identity, and μ_f the dynamic viscosity.

As for the structure part, the elasticity equation with the St. Venant Kirchhoff material model is used. Let X be the reference configuration and $x = \chi(X,\ t)$ the position in the current configuration. The structure part of the coupled problem can be denoted as

$$\nabla \cdot \left(FS^T\right) + \rho_s f_s = \rho_s \ddot{\chi} \quad \text{in } \Omega_s \quad (4)$$

with f_s the outer forces acting on the structure, ρ_s the structure density,

$$S = \lambda_s tr\left(E\right) I + 2\mu_s E \quad \text{in } \Omega_s \quad (5)$$

the second Piola-Kirchhoff stress tensor, λ_s, and μ_s the Lam constants,

$$E = \frac{1}{2}\left(F^T F - I\right) \quad \text{in } \Omega_s \tag{6}$$

the Green-Lagrange strain,

$$F = \frac{\partial \chi}{\partial X} \quad \text{in } \Omega_s \tag{7}$$

the deformation gradient, and

$$v_s = \dot{\chi} \quad \text{in } \Omega_s \tag{8}$$

the structure velocity. The FSI boundary conditions for fluid and structure on Γ then follow as

$$v_f = v_s \quad \text{and} \quad \frac{1}{\det\left(F\right)} FSF^T n_s = \sigma_f n_f. \tag{9}$$

3. EXTRAPOLATION IN FSI

Let $(\phi)_i^n$ be the discrete counterpart to a time and space dependent variable ϕ at FSI iteration i, at time step n and ϵ_{FSI} the FSI convergence criterion.

3.1. NATIVE FSI ALGORITHM

One time step of the native partitioned implicit FSI implementation is depicted in figure 1. The ith iteration of the nth time step can be described as follows. First the Navier-Stokes equation is solved for velocity and pressure $(v)_i^n$, $(p)_i^n$ in the fluid domain. Using this solution

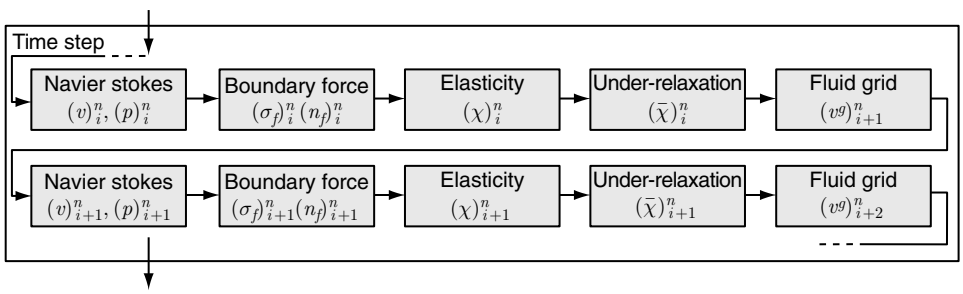

Figure 1 Native implicit partitioned FSI algorithm.

the force on the FSI boundary $(\sigma_f)_i^n$ $(n_f)_i^n$ is derived. Implementing the force as boundary condition, the elasticity equation is solved for the displacement $(\chi)_i^n$ on the structure domain. Then the procedure checks for convergence. If $i \neq 1$ and

$$\frac{\left\|(\chi)_i^n - (\chi)_{i-1}^n\right\|^2}{\left\|(\chi)_i^n\right\|^2} < \epsilon_{FSI}, \tag{10}$$

FSI convergence is achieved and the next time step is calculated. Otherwise, the structure solution is under-relaxed by a constant under-relaxation factor α:

$$(\bar{\chi})_i^n = \alpha(\chi)_i^n + (1-\alpha)(\chi)_{i-1}^n. \tag{11}$$

Then, the fluid grid is displaced according to $(\bar{\chi})_i^n$ and a new grid velocity $(v^g)_{i+1}^n$ in the fluid domain as well as a new fluid boundary condition on Γ is computed.

3.2. EXTRAPOLATION FUNCTIONS

Extrapolation is a well known technique to accelerate many kinds of unsteady processes, as it can provide a sophisticated initial guess to the underlying solver. In implicit partitioned FSI computations it is mainly used in two areas. Either it is applied within a time step, i.e. as vector extrapolation (see U. Küttler and W. Wall [6]), or to generate a more promising initial structural displacement in the current time step using polynomial extrapolation as in J. Vierendeels et al. [13] or M. Schäfer et al. [9].

As polynomial extrapolation functions have been proven of value in this field, see [2, 11, 3, 14], they are also used in this work. To demonstrate the effect of different orders of extrapolation, four different orders are implemented, namely the first four Lagrange polynomial interpolation functions.

Let $(\phi)_*^n$ be the state of variable (ϕ) at FSI convergence in time step n. Then the Lagrangian interpolation functions state:

$$\text{0th order :} \qquad \phi_1^n = \phi_*^{n-1} \tag{12}$$

$$\text{1st order :} \qquad \phi_1^n = 2\phi_*^{n-1} - \phi_*^{n-2} \tag{13}$$

$$\text{2nd order :} \qquad \phi_1^n = 3\phi_*^{n-1} - 3\phi_*^{n-2} + \phi_*^{n-3} \tag{14}$$

$$\text{3rd order :} \qquad \phi_1^n = 4\phi_*^{n-1} - 6\phi_*^{n-2} + 4\phi_*^{n-3} - \phi_*^{n-4}. \tag{15}$$

These functions are used for both displacement and force extrapolation. Higher order extrapolation suggest a higher order of accuracy, thus less iterations to convergence, however, their implementation requires more memory and computing time.

3.3. EXTRAPOLATED DISPLACEMENT

In the case of displacement extrapolation the structural displacement χ on Γ is altered in the first FSI iteration of every time step. Singly the variables on the FSI boundary, as opposed to the entire fluid region Ω_f, are extrapolated in order to minimize memory consumption. The course of this algorithm in time step n is depicted in figure 2.

In contrast to the native algorithm, the fluid solution, derivation of force on the boundary, and solution of the structure problem are skipped. Instead, the first structure solution $(\chi)_1^n$ is extrapolated by one of the equations (12) to (15). Additionally, no under-relaxation is applied to the displacements, as this would damp the advantage of extrapolation. The following iterations are carried out according to the non-extrapolated case.

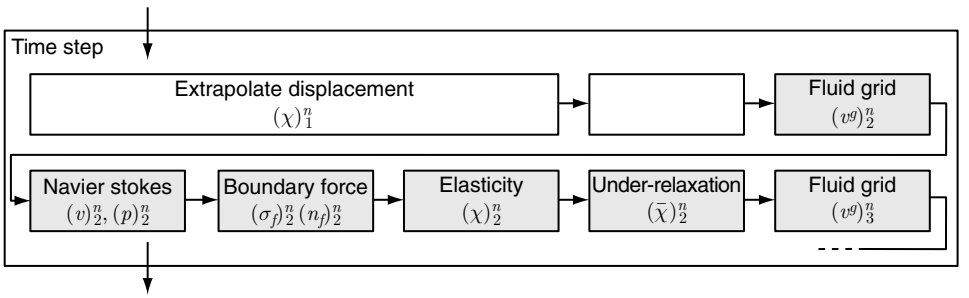

Figure 2 FSI algorithm with displacement extrapolation.

3.4. EXTRAPOLATED FORCE

In the case of fluid force extrapolation, the boundary forces $\sigma_f n_f$ on Γ acting on the structure are extrapolated. This affects the FSI procedure in the same way as extrapolating the fluid variables v and p on the entire domain Ω_f, but saves memory, as singly values on the interface have to be stored. A sketch of this algorithm in time step n is given in figure 3.

Here, the first FSI iteration omits the fluid solution and the derivation of force on the FSI boundary. In this case, the force $(\sigma_f)_1^n (n_f)_1^n$ is extrapolated by one of the equations (12) to (15). Once again the under-relaxation of the structure solution is omitted in the first iteration, as for the displacement case.

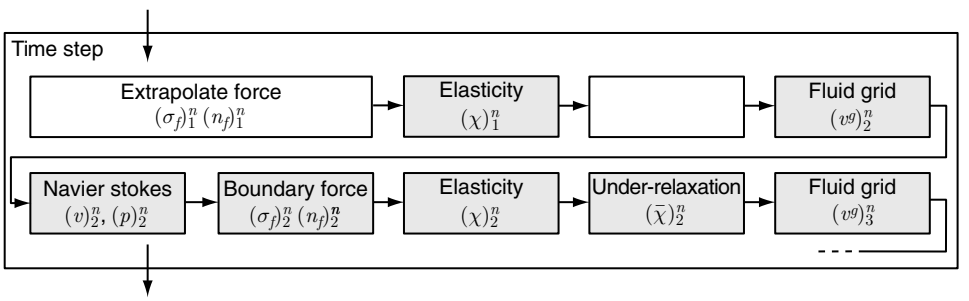

Figure 3 FSI algorithm with force extrapolation.

Again, the following iterations are identical to the non-extrapolated case. Compared to the displacement extrapolation this introduces an additional structure solve per time step. However, the gain in accuracy outweighs this additional solve in terms of CPU time needed for convergence.

4. SOLVERS

The fluid structure coupling is realized by an implicit partitioned approach. under-relaxation is applied to the structural displacements by a constant Under-relaxation factor. This ensures that the acceleration of the FSI procedure originates singly from the initial guess in every time step, thus the applied extrapolation.

The fluid is solved by the in house finite volume code FASTEST [4]. It utilizes the SIMPLE algorithm by S.V. Patankar and D.B. Spalding [7], the linearized fix point problem is solved using an incomplete ILU factorization and a geometric multi grid is implemented to accelerate the procedure. The code operates on block structured hexahedral grids. As for time stepping, a second order backwards difference scheme is used.

The non-FSI grid boundaries are moved by interpolating splines and a transfinite interpolation scheme is used to smooth the inner-block grids.

The structure problem is solved by the finite element code FEAP by R. L. Taylor [10]. It uses Newton iteration and the resulting linear system is solved by a conjugate gradient solver. The second order transient Newmark scheme is used for temporal integration.

The coupling and exchange of forces and displacements on the non-matching grids is realized by the code coupling interface MpCCI [1].

5. BENCHMARK TEST CASE

A commonly used FSI test case is chosen to compare the different approaches described above. This test case consists of a channel flow around a rigid cylinder with an elastic bar attached to it. All parameters are set according to the FSI Benchmark by S. Turek et al. [12].

The channel has the dimensions 2.5×0.41 m^2, with a slightly off symmetric positioned cylinder at (0.2 m, 0.2 m), radius 0.05 m and a bar attached to the cylinder of size 0.35×0.02 m^2. Figure 4 shows the configuration, with its fluid and structure domain. Boundary conditions for the fluid are: A parabolic inflow profile

$$v_f\Big|_{\text{Inlet}} = 1.5\,\bar{v}\left(\frac{4.0}{0.1681}\frac{y}{m}\left(0.41-\frac{y}{m}\right),\ 0\right)^T, \tag{16}$$

with $\bar{v} = 2$ m/s, zero-gradient outlet condition, and no-slip on all other surfaces. The structure is clamped at the cylinder. The fluid field is initialized with constant velocity $v_f = (\bar{v}, 0)^T$, the structure is initially at rest without any loading.

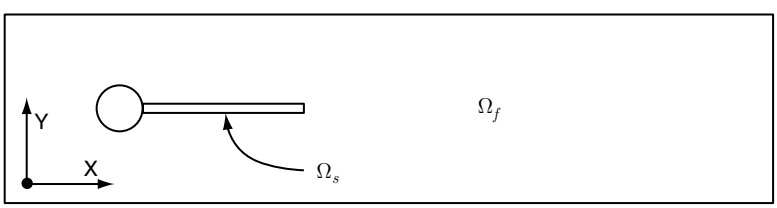

Figure 4 Sketch of the fluid and structure domain of FSI 3.

The fluid is set to be incompressible and Newtonian with density $\rho = 1{\cdot}10^3$ kg/m^3 and dynamic viscosity $\mu_f = 1$ kg/ms. This leads to a Reynolds number of Re = 200. The structure is described by the St. Venant Kirchhoff model with density $\rho = 1{\cdot}10^3$ kg/m^3, $\lambda_s = 8{\cdot}10^6$ kg/ms^2, and $\mu_s = 2{\cdot}10^6$ kg/ms^2.

6. NUMERICAL RESULTS

The objective of this work is to compare the different extrapolation algorithms with respect to numerical efficiency. All tests were calculated on the same grid with fixed under-relaxation parameter and solver parameters. The comparison involves 0.5 seconds of physical time with three different time step sizes $\Delta t = 0.001$ s, 0.002 s, and 0.005 s. 0th to 3rd order extrapolation is used for the displacement and force cases. The computational domain is discretized into 64 elements for the structure and 15,856 volumes for the fluid in 2D. The third space dimension is discretized by 2 elements in the structure and 4 volumes in the fluid. Additional boundary conditions for the third dimension are zero-gradient for the structure and periodicity for the fluid. Figure 5 shows a section of the non-matching computational grids after 0.05 and 0.15 seconds. Computations were carried out on an Intel Core i7 (2.8 GHz).

The measurement starts with a fully developed flow field and the bar moving in constant cycles. The bar tip displacement for time step $\Delta t = 0.001$ s is shown in figure 6. The force acting on the FSI boundary is shown in figure 7. Their mean values are shown in tables 1 and 2. Comparing the largest time step $\Delta t = 0.005$ to the smallest time step $\Delta t = 0.001$, the relative error in tip displacement is 0.58% in amplitude and 1.77% in wavelength, the relative error in drag amplitude is 0.15% and 0.47% in wavelength, and the relative error in lift amplitude is 0.85% and 2.23% in wavelength.

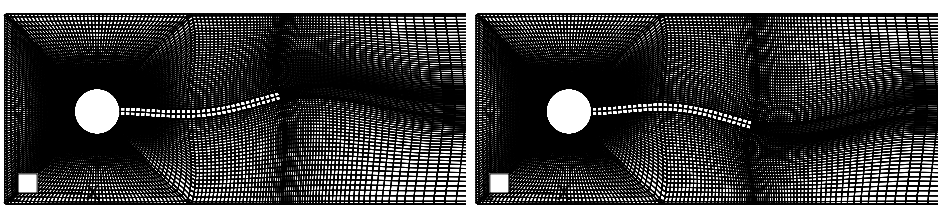

Figure 5 Section of the fluid and structure grid.

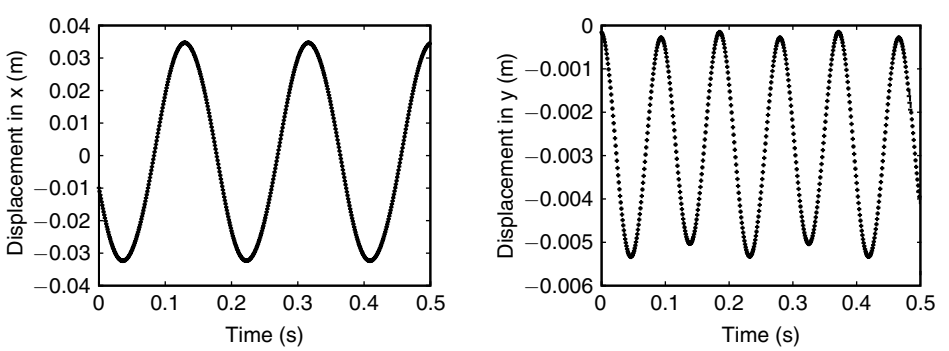

Figure 6 Bar tip movement with time step size $\Delta t = 0.001$ s.

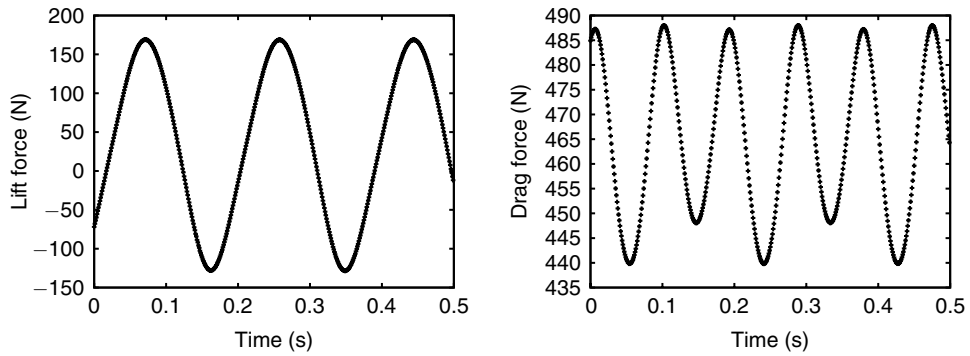

Figure 7 Force on Γ with time step size $\Delta t = 0.001$ s.

Table 1 Average bar tip displacement

Time step [s]	x**-displ. [m]**	x**-freq. [1/s]**	**Displ.** y **[m]**	y**-freq. [1/s]**
0.001	–0.0027 ± 0.0026	10.72	0.0012 ± 0.0335	5.35
0.002	–0.0027 ± 0.0026	10.70	0.0012 ± 0.0335	5.38
0.005	–0.0027 ± 0.0026	10.53	0.0012 ± 0.0333	5.41

Table 2 Average force on acting on Γ

Time step [s]	**Drag [N]**	**Drag freq. [1/s]**	**Lift [N]**	**Lift freq. [1/s]**
0.001	463.90 ± 24.11	10.72	20.18 ± 148.80	5.38
0.002	463.88 ± 23.94	10.70	20.05 ± 148.78	5.32
0.005	463.80 ± 23.46	10.67	19.74 ± 147.80	5.26

Figures 8, 9, and 10 show the average CPU times per time step. The native FSI algorithm coincides with the 0th order displacement extrapolation, as the new time step starts its calculation on the grid displaced in the last time step.

As expected, all extrapolation algorithms show faster convergence than the native FSI algorithm. The force case outperforms the displacement case for small orders of extrapolation independent of the time step size.

For small time step sizes the CPU time needed for the displacement case approaches the time needed for the force case as the order of extrapolation increases. This behavior reduces with increasing time step size. The advantage of force over displacement extrapolation is clearly seen at the largest time step $\Delta t = 0.005$ s. There, the maximum improvement of the displacement extrapolation is reached at 3rd order. This is more than 2 times slower than the 3rd order force extrapolation.

For $\Delta t = 0.005$ s the 3rd order force extrapolation is more than 2.5 times faster than the native algorithm.

The maximum improvement for time step $\Delta t = 0.002$ s shows the 2nd order force extrapolation, which is more than 3 times faster than the native algorithm. The fastest displacement case is at 3rd order extrapolation.

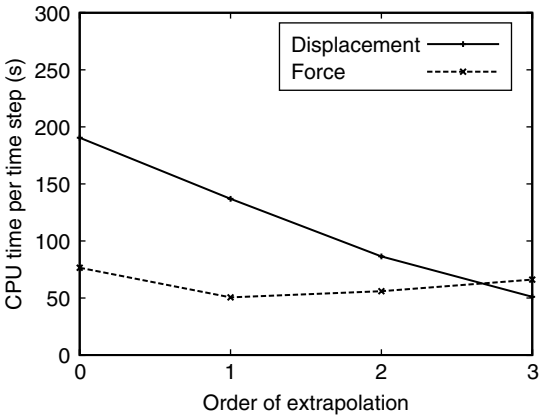

Figure 8 Average CPU time for one time step $\Delta t = 0.001$.

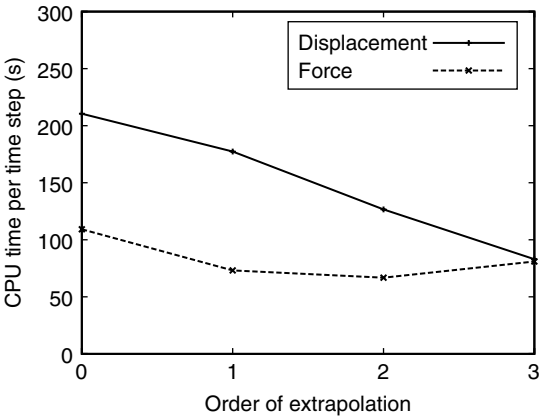

Figure 9 Average CPU time for one time step $\Delta t = 0.002$.

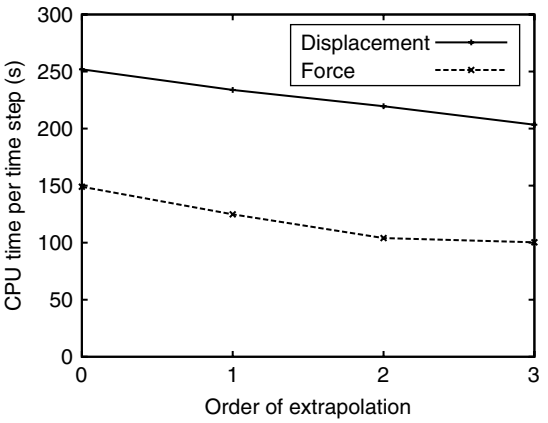

Figure 10 Average CPU time for one time step $\Delta t = 0.005$.

For the time step Δt = 0.001 s the maximum improvement can be seen with the 1st order force extrapolation, which is more than 3.7 times faster than the native algorithm. The best convergence for the displacement case can be found with 3rd order extrapolation.

7. CONCLUSIONS

In this article the extrapolation of forces acting on the structure at the FSI boundary in order to accelerate unsteady implicit partitioned FSI computations is described and examined. This is compared to the well known acceleration technique of extrapolating the displacement on the FSI boundary. Numerical tests based on an FSI Benchmark show the superior performance of the force extrapolation for different time step sizes. This advancement can be achieved at minimal computational cost as the same memory blocks and extrapolation procedures as for the displacement extrapolation can be employed.

In addition, different extrapolation schemes based on the Lagrange interpolation polynomials are compared. It is shown that the impact of a higher degree of extrapolation is increasing with the time step size. This leads to more efficient implicit solvers, as greater time step sizes can be used and less FSI iterations per time step are needed.

As for future prospects, the combination of force extrapolation with other extrapolation techniques can be studied. Furthermore, this approach can be combined with other acceleration methods acting within single time steps. As these two kinds of methods are completely independent a superposition of speedup is expected.

ACKNOWLEDGMENT

The work of Stephen Sachs is supported by the ‘Excellence Initiative’ of the German Federal and State Governments and the Graduate School of Computational Engineering at Technische Universität Darmstadt.

REFERENCES

[1] Fraunhofer Institute Algorithms and Scientific Computing. MpCCI 3.0.6 Documentation, 2007.

[2] M. Breuer and M. Münsch. FSI of the turbulent Flow around a Swiveling Flat Plate Using Large-Eddy Simulation. In Stefan Hartmann, Andreas Meister, Michael Schäfer, and Stefan Turek, editors, *International Workshop on Fluid-Structure Interaction – Theory, Numerics and Applications*, pages 31–43, 2008.

[3] M. Breuer and M. Münsch. LES meets FSI – Important Numerical and Modelling Aspects. In V. Armenio et al., editors, *Direct and Large Eddy Simulations VII*, ERCOFTAC. Springer Science+Business Media B.V., 2010.

[4] Technische Universität Darmstadt Fachgebiet Numerische Berechnungsverfahren im Maschinenbau. FASTEST User Manual, 2005.

[5] Ulrich Küttler and Wolfgang Wall. Fixed-point fluid-structure interaction solvers with dynamic relaxation. *Computational Mechanics*, 43(1): 62–72, 2008.

[6] Ulrich Küttler and Wolfgang Wall. Vector Extrapolation for Strong Coupling Fluid-Structure Interaction Solvers. *Journal of Applied Mechanics*, 76(2): 021205, 2009.

[7] S.V Patankar and D.B Spalding. A calculation procedure for heat, mass and momentum transfer in three-dimensional parabolic flows. *International Journal of Heat and Mass Transfer*, 15(10): 1787–1806, 1972.

[8] Serge Piperno. Explicit Implicit fluid structure staggered procedures with a structural predictor and fluid subcycling for 2d inviscid aeroelastic simulations. *International Journal for Numerical Methods in Fluids*, 25(10): 1207–1226, 1997.

[9] M. Schäfer, D. C. Sternel, G. Becker, and P. Pironkov. Efficient Numerical Simulation and Optimization of Fluid-Structure Interaction. In *Fluid Structure Interaction II: Modelling, Simulation, Optimization*, volume 73, pages 131–158. Springer, 2010.

[10] Robert L. Taylor. FEAP – A Finite Element Analysis Program, 2008.

[11] Tayfun E. Tezduyar, Matthew Schwaab, and Sunil Sathe. Sequentially-Coupled Arterial Fluid-Structure Interaction (SCAFSI) technique. *Computer Methods in Applied Mechanics and Engineering*, 198(45–46): 3524–3533, 2009.

[12] Stefan Turek and Jaroslav Hron. Proposal for Numerical Benchmarking of Fluid-Structure Interaction between an Elastic Object and Laminar Incompressible Flow. In Hans-Joachim Bungartz and Michael Schäfer, editors, *Fluid-Structure Interaction*, volume 53 of *Lecture Notes in Computational Science and Engineering*, pages 371–385. Springer Berlin Heidelberg, 2006.

[13] Jan Vierendeels, Lieve Lanoye, Joris Degroote, and Pascal Verdonck. Implicit coupling of partitioned fluid-structure interaction problems with reduced order models. *Computers & Structures*, 85(11–14): 970–976, 2007.

[14] Wolfgang A. Wall, Axel Gerstenberger, Peter Gamnitzer, Christiane Förster, and Ekkehard Ramm. Large Deformation Fluid-Structure Interaction – Advances in ALE Methods and New Fixed Grid Approaches. In Hans-Joachim Bungartz and Michael Schäfer, editors, *Fluid-Structure Interaction*, volume 53 of *Lecture Notes in Computational Science and Engineering*, pages 195–232. Springer Berlin Heidelberg, 2006.

[15] Saim Yigit, Marcus Heck, Dörte Carla Sternel, and Michael Schäfer. Efficiency of Fluid-Structure Interaction Simulations with Adaptive Underrelaxation and Multigrid Acceleration. *International Journal of Multiphysics*, 1(1): 85–99, 2007.